ACS APPLIED MATERIALS & INTERFACES

Research Article

www.acsami.org

Controlling Formation of Silver/Carbon Nanotube Networks for Highly Conductive Film Surface

Rui-Xuan Dong,[†] Chung-Te Liu,[†] Kuan-Chieh Huang,[‡] Wen-Yen Chiu,[†,‡] Kuo-Chuan Ho,[†,‡] and Jiang-Jen Lin*[,†]

[†]Institute of Polymer Science and Engineering and [‡]Department of Chemical Engineering, National Taiwan University, Taipei 10617, Taiwan

Supporting Information

ABSTRACT: Flexible polymer films with high electrical conductivity were prepared through a simple coating of well-dispersed silver nanoparticle (AgNP) and multiwalled carbon nanotube (CNT) solution. The hybrid film with surface resistance as low as 1×10^{-2} Ω/sq was prepared by controlling the annealing temperature in air and by using a suitable composition of silver nitrate/CNT/poly(oxyethylene)-oligo(imide) (POE-imide) in the ratio 20:1:20 by weight. During the heating, color of the film surface changed from black to golden to milky white, indicating the accumulation of AgNPs through surface migration and melting into CNT-connected networks. Thermogravimetric measurements showed that the transition temperature of 170 °C was responsible for the POE-imide degeneration and the subsequent Ag melting with a decrease in the surface resistance from 2.1×10^{5} to 2.0×10^{-1} Ω/sq, which was able to illuminate light-emitting diode lamps because of the formation of a continuous Ag network.

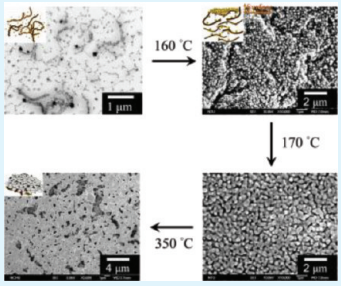

KEYWORDS: *carbon nanotube, silver melting, nanohybrid, conductivity, thermal degradation*

INTRODUCTION

Electrically conductive materials, including organic conducting polymers (CPs), inorganic metals, and carbon nanotubes (CNTs), have been extensively studied because of their potential applications in the electronics and automotive industries.[1−3] However, each conductive material has its limitations in terms of fabrication into a practical and large-scale conductor or device. It should be noted that the sheet resistances of organic CP have reached a maximum of ca. 1 Ω/sq. Further, conductivity value as high as 1×10^{3} to 1×10^{6} S/cm have been recorded for single- and multiwalled CNTs with lengths of 100−1000 μm.[4−7] However, CNTs generally exist as aggregates because of bundling entanglement brought about by intense van der Waals interactions. Moreover, the difficulty in generating a homogeneous dispersion of CNT in organic media still hinders their use in many practical applications. Perhaps the most widely used method to overcome this limitation involves the ultrasonication-enforced segregation of nanotube strands out of entangled bundles, followed by noncovalent or covalent modification of the chemical functionality of the CNT surfaces. Noncovalent strategies are required to disperse CNTs in organic media in order to preserve their excellent electrical and structural properties; to this end, a wide range of surfactants,[8,9] small molecules,[10,11] and polymers[12−15] have been used. Among these agents, polymers are capable of forming new functional materials through well-defined CNT/polymer interactions. In particular, flexible and conjugated polymers provide structures capable of wrapping the surfaces of CNT, which facilitates their dispersion in organic media.[16−18] These hybrid polymers often exhibit synergistic optoelectronic effects with striking variations in electrical conductivity at percolation thresholds[19] ranging from 0.0025 wt %[20] to several mass percentages.[21−23] The conductivity values are similar, often remaining below 10^{-1} S/cm. These effects result from the process of dispersing CNT, as sonication can cause significant damage by producing defects and severing the CNT.[24,25] In addition, when CNT form a connective network within a polymer matrix, the presence of an insulating polymer layer at each CNT−CNT junction prevents direct contact between the CNTs.[26,27] Thus, the conductivity of a composite is much lower than that of a well-connected network of neat CNTs. To achieve conductivity that is an order of magnitude higher, researchers have investigated the decoration of CNTs with metal nanoparticles through a wet chemistry reaction with the aim of enhancing the conductivity and reducing the contact resistance of CNT junctions in a polymer matrix.[28−30]

Silver nanoparticles (AgNPs) have the potentials for electric conductor uses[31,32] besides their catalytic[33] and antimicrobial[34] properties. However, the presence of added silver flake in mixing with AgNPs was required to fabricate a conductive film. The low melting temperature at 178 °C was reported.[31,32] Silver is known to be an optimum metal in microelectronics industries because it has the highest electrical conductivity (6.3×10^{5} S/cm) among all metals.[35] For a typical representative research work, it is difficult to fabricate silver-coated polymer films with a low electrical resistance (<0.1 Ω/sq).[36−38] In particular, their fabrication is usually unstable, and therefore, these films warrant fresh

Received: December 1, 2011
Accepted: February 2, 2012
Published: February 2, 2012

preparation via high-temperature thermal treatment (>300 °C) to realize the formation of a network of silver-coated polymer films. Because of the above-mentioned limitations, current research on conductive AgNPs/polymer films is focused on the synthesis of silver melt by using the hydrothermal process as that described in the literature.[39−41] Our research group has shown the silver melt to have a low melting temperature of 110 °C on the surface of clay and the melting temperature is a function of the particle size.[42] Because of the fact that the silver content is too low to continue the formation of a network with silver-coated films, the surface conductivity of the films does not increase further. Therefore, we have reported an easy process and direct heating method to produce a highly concentrated homogeneous Ag/CNT solution at high concentration in mixed organic medium using a copolymer as a dispersant and a reducing agent. The requisite poly(oxyethylene)-oligo(imide) (POE-imide) was prepared previously from an aromatic dianhydride and poly(oxyethylene)-amine at an equivalent ratio of 5:6 and allowed the CNT aggregates to debundle into individual tubes[43] and further interact homogeneously with the $AgNO_3$ and consequently reduced AgNPs. Then, van der Waals forces induced the deposition of AgNPs with diameters of 8−30 nm on the CNT surface that remained highly stable without obvious sedimentation for long-term storage.

In this work, we present a detailed study of the influence of melting AgNPs on the electrical resistance of POE-imide/CNT films generated through consecutive procedures of CNT dispersion, $AgNO_3$ reduction, solution casting and thermal treatment in air. The generated Ag/CNT films were characterized in terms of their surface and sheet resistance. Further, these films had a sheet resistance of 2.0×10^{-1} Ω/sq owing to the presence of the silver melt at 170 °C on their surface; this value of sheet resistance is, to the best of our knowledge, the lowest reported for a polymer film with Ag/CNT.

MATERIALS AND METHODS

Materials. Multiwalled CNT with 95% purity and containing 5% catalyst (Fe, Co, and Ni) were obtained from Seedchem Company Pty., Ltd. The average dimensions for individual CNTs were 40−60 nm in diameter and 0.5−10 μm in length. The oligomer dispersant, POE-imide, was synthesized from the reaction of polyether diamine and dianhydride through previously reported procedures.[43] Poly(oxyethylene)-diamine or poly(oxypropylene-oxyethylene-oxypropylene)-block polyether of bis-(2-aminopropyl ether) of averaged 2000 g/mol (POE2000) is a water-soluble and crystalline POE-backboned amine (waxy solid, mp 37−40 °C, amine content 0.95 mequiv/g with an average of 39 oxyethylene and 6 oxypropylene units in the structure), purchased from Huntsman Chemical Co. The anhydride, 4,4′-oxidiphthalic anhydride (ODPA, 97% purity), was purchased from Aldrich Chemical Co. and sublimed. $AgNO_3$ (99.8%) and sodium borohydride ($NaBH_4$, 97%) were purchased from SHOWA Chemical Co. Tetrahydrofuran (THF) and *N*,*N*-dimethylformamide (DMF) were purchased from TEDIA Company Inc.

Preparation of Poly(oxyethylene)-oligo(imide) (POE-imide). The typical experimental procedures for synthesizing the POE-imide dispersant are described below for the oligomer with the composition of POE2000 and ODPA at a 6:5 equivalent ratio. To a 100 mL three-necked and round-bottomed flask equipped with a magnetic stirrer, nitrogen inlet−outlet lines, and a thermometer was added POE2000 (10.0 g, 0.005 mol) in THF (15 mL), followed by a solution of ODPA (1.29 g, 0.0042 mol) in THF (10 mL) through an addition funnel in a dropwise manner. During the addition, the mixture was stirred vigorously and the reaction temperature was maintained at 150 °C for 3 h. The product mixture was subjected to rotary evaporation under a reduced pressure and recovered as a yellowish waxy solid. During the process, samples were taken periodically and monitored using a FT-IR. This showed that the absorption peaks of anhydride functionality at 1780 cm^{-1} (s) and 1850 cm^{-1} (w) disappeared at the expense of the peaks at 1713 and 1773 cm^{-1} for the asymmetric stretch of imide. The characteristic absorption at 1100 cm^{-1} of oxyalkylene was observed.

Preparation of POE-imide Nanohybrids with Ag/CNT. The nanohybrids of AgNPs decorated on the CNT surface were synthesized by an in situ reduction of $AgNO_3$ in the presence of polymer dispersed CNTs. CNT (0.025 g) were first dispersed in 5 mL of DMF in a vial and sonicated under a VCX 500 Ultrasonicator at ambient temperature for 10 min. The resultant solution was dark black with some solid precipitates at the bottom of the container, indicating a low degree of dispersion. In a separate glass container, POE-imide (0.5 g) and $AgNO_3$ (0.5 g, 0.003 mol) were dissolved in 5 mL of deionized water (R = 18.2 M Ω/cm^2) and added to the CNT/DMF (5.0 mL) solution. A homogeneous suspension of CNTs was obtained by simple mixing in the presence of POE-imide and $AgNO_3$. This mixture was continuously stirred for several days at ambient temperature and the apparent color changes monitored using a UV−visible (UV−vis) spectrophotometer. It was observed that there was a color change from black to black-brownish and surface plasma resonance peak at 400 nm, corresponding to the out-of-plane dipole resonance of silver nanospheres, indicating a reduction of Ag^+ to Ag^0. Two controlled experiments were performed for the combination of CNT/$AgNO_3$ without dispersant and $AgNO_3$ with dispersant only; CNT (0.025 g) and $AgNO_3$ (0.5 g, 0.003 mol) dissolved in DMF/water mixture and $AgNO_3$ (0.5 g, 0.003 mol) and POE-imide (0.5 g) in the solution without CNT under the standard conditions for silver reduction.

Preparation of Ag/CNT Nanohybrid Films. In this study, conductive films were prepared by a casting method. Typically, the matrix could be rigid (e.g., glass) or flexible (e.g., polyimide (PI)) film depending on the field of application. The PI film (2 cm × 2 cm, see Figure 1) was washed several times with ethanol and used as the substrate. The Ag/CNT solution (0.5 g) was cast on a piece of the PI film; the film was then placed in a high-temperature oven with the heating program set as follows: 110, 160, 170, 300, and 350 °C for each 20 min. Finally, flexible and conductive films were fabricated and then characterized.

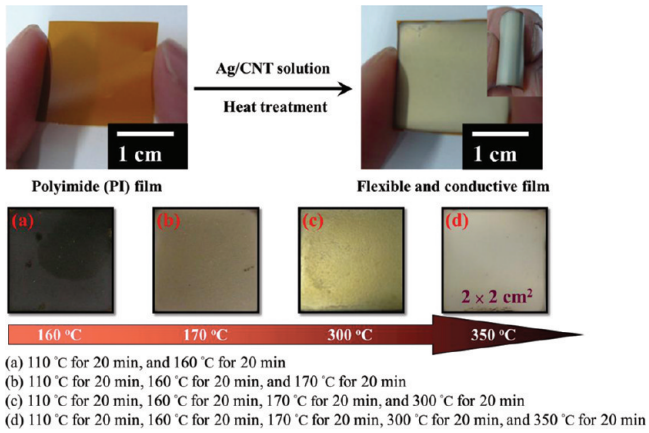

Figure 1. Photographs of melting AgNPs on the surface of polyimide film during the heating treatment. (a) 160 °C after 20 min, (b) 170 °C after 20 min, (c) 300 °C after 20 min, and (d) 350 °C after 20 min.

Instruments and Analyses. The dispersion of Ag/CNT solution was examined using a transmission electron microscope (TEM, JEOL JEM-1230), which is equipped with an electron microscope operating at 100 kV, and photographed using a Gatan Dual Vision CCD camera. The samples were prepared by dropping the sample solution on to copper grids coated with a carbon film. Surface resistance measurements for the film containing AgNP were performed with a Keithley 2400 digital sourcemeter equipped with a four-point probe. A demo of LED lamps (power dissipation = 100 mW, peak forward current = 100 mA) were designed to show the conductive ability. Variations in the melting of silver samples were observed by examining the surface

Table 1. Sheet Resistance of the Films Prepared from the CNT/Ag/Polymer Nanohybrids

sample[a]	weight fraction (w/w/w)	sheet resistance (Ω/sq)[c] 160 °C	170 °C	300 °C	350 °C
pristine CNT[b]	1	1.7×10^1	1.7×10^1	1.7×10^1	1.7×10^1
CNT/POE-imide	1/1	6.6×10^2	5.5×10^2	4.8×10^2	4.5×10^2
	1/10	4.2×10^3	1.8×10^3	1.3×10^3	4.7×10^2
	1/20	2.1×10^6	1.7×10^6	8.2×10^5	6.2×10^2
$CNT/AgNO_3$	1/20	[e]	[e]	[e]	[e]
$CNT/AgNO_3$/POE-imide	1/10/10	5.2×10^5	1.3×10^2	9.5×10^1	2.4×10^0
	1/20/20	2.1×10^5	2.0×10^{-1} (8.7×10^6)[d]	1.1×10^{-1}	1.0×10^{-2} (9.1×10^2)[d]
	1/40/40	2.5×10^5	3.7×10^1	5.2×10^0	9.8×10^{-1}
$AgNO_3$/POE-imide	1/1	1.0×10^5	1.3×10^3	9.3×10^1	8.2×10^0

[a]Solution coating on polyimide (PI) film. [b]17.1 Ω/sq at room temperature. [c]Measured by using a four-point probe. [d]The sheet resistance of bottom layer. [e]Incomplete film and the resistance is similar to pristine PI film (1×10^{-12} Ω/sq).

and fracture morphologies of the nanocomposite films using a field-emission scanning electronic microscope (FE-SEM, Zeiss EM 902A), at 80 kV. Furthermore, the morphology of the Ag/CNT nanohybrid films on the PI substrate was analyzed using a tapping-mode atomic force microscope (TM-AFM, Seiko SPI3800N, Series SPA-400HV; cantilever type: SI-DF20, f = 139 kHz, spring constant =16 N m^{-1}). Normal characterization of the composition of the nanocomposite films requires measurements of wide-angle X-ray diffraction (WAXRD); these measurements were performed at a scanning rate of 2° min^{-1} using a Rigaku D/MAX-3C OD-2988N X-ray diffractometer with a copper target and a Ni filter. The organic content was estimated using a thermal gravimetric analyzer (TGA, Perkin-Elmer Pyris 1) with a temperature gradient that ramped from ambient temperature to 900 °C at a rate of 10 °C min^{-1} in air.

RESULT AND DISCUSSION

Synthesis of POE-imide Dispersant for Ag/CNT Nanohybrids. The requisite POE-imide was prepared by the imidation of POE2000 and ODPA in a molar ratio of 6:5 at a temperature of 150 °C. The polymeric dispersant consisted of alternating POE $-(CH_2CH_2O)_x-$ and aromatic imide $-(CONCO)-$ segments that were allowed to unbundle the CNT aggregates into individual tubes and further interact homogeneously with the in situ generated AgNPs. It was observed that some AgNPs were deposited on the CNT surface through the noncovalent van der Waals force while other free AgNPs remained in solution (see the Supporting Information, Figure S1). The difference in the geometric shape between the two materials and the noncovalent bonding interaction involving the imide functionalities $-(CONCO)-$ and POE $-(CH_2CH_2O)_x-$ groups present a unique method of preparing either the Ag/CNT nanohybrid dispersion or a homogeneous solution containing AgNPs. By comparison, the homogeneous AgNPs can be prepared first and deposited on to the second nanomaterial. In fact, the reduction of $AgNO_3$ with $NaBH_4$ in the presence of POE-imide also produced a homogeneous dispersion of AgNPs that were 10−30 nm in diameter. However, when the dispersed AgNPs was introduced into the CNT slurry, the CNT remained aggregated rather than being unbundled, whereas the interaction with AgNPs was weak.

Preparation of Ag/CNT/POE-imide Films. The conductive films were fabricated by casting the nanohybrid dispersion on the PI matrix and then placing this matrix in a high-temperature oven with the heating program set as follows: 110, 160, 170, 300, and 350 °C for 20 min at each temperature. The functions of CNTs were to provide a solid surface for $AgNO_3$ to adhere through adsorption and to subsequently serve as two-dimensional templates for noncovalent bonding with AgNPs. When samples of Ag/CNT were solution-coated onto PI slides and continuously heated at temperatures higher than 170 °C for 20 min, flexible and conductive films were prepared. During this process, the color of the film surface changed from black to golden to milky white as the temperature was increased from 160 to 170 and finally to 350 °C, respectively (Figure 1a, b, and d). These changes in the color of the film surface are expected to be caused by the migration, aggregation, and variation in the dimensions of AgNPs. The role of the CNTs was demonstrated through control experiments. In the absence of CNTs, a reduction in the amount of $AgNO_3$ resulted in the generation of AgNPs that showed a consistent blackish-green color during thermal treatment, and the electrical behavior of $AgNO_3$ was inferior to that of pristine CNT. The sheet resistance of the polymer films could be decreased by blending CNTs. The sheet resistances of hybrid films at different CNT concentrations are listed in Table 1. The sheet resistance in the unit of Ω/sq was directly monitored by a four-point probe, which could avoid the error of measuring the film thickness.[36−38] When the percolation threshold was reached, the nanotubes formed a conductive path through the PI matrix. At this critical concentration, i.e., at 10 wt % CNTs, the surface resistance drastically decreased by 3 orders of magnitude from 1×10^6 to 1×10^3 Ω/sq. In one example at low CNT loading (5 wt %), a conductive CNT network failed to form in the POE-imide matrix. Although the hybrid was further heated at 170 °C for 20 min, the CNTs were still wrapped by an organic dispersant and the sheet resistance of the hybrid remained very close to that of the pure POE-imide matrix. Among these nanohybrids, when the CNT:$AgNO_3$ weight ratio was 1:20 without using POE-imide, a silver mirror appeared on the side of the reactor wall due to the formation and inhomogeneous aggregation of AgNPs from the solution. It is necessary to have the presence of POE-imide as the suitable stabilizer in order to generate a homogeneous Ag/CNT solution. The use of an appropriate composition allowed the coated surface to exhibit a reduction of in the sheet resistance of approximately 7 orders of magnitude (from 2.1×10^5 to 1.0×10^{-2} Ω/sq), depending on the heat treatment. This value of electrical resistance is much lower than that of CNT/polymer and AgNP/polymer composites and, to the best of our knowledge, of Ag/CNT nanohybrid films. The experiment of further increasing silver or decreasing CNT concentration as in CNT:$AgNO_3$ weight ratio of 1:40 showed a higher resistance due to the apparent Ag aggregation in solution. Hence, the proper amount of CNTs could be considered as suitable dispersants and scaffolds for directing the AgNP migration into surface and attaching the structure of one-dimensional conductive film. Furthermore, this change in surface resistance could be used to illuminate light-emitting diode (LED) bulbs, as shown in Figure 2. When the Ag/CNT mixture was

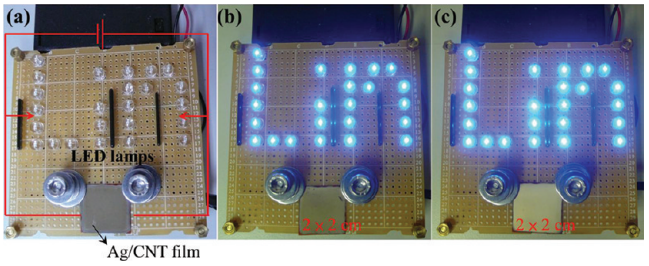

Figure 2. Demonstration of conductive application by heating Ag/CNT films at (a) 160, (b) 170, and (c) 350 °C, respectively.

heated at a temperature less than 170 °C, the surface resistance was too high to illuminate the LED lamps (Figure 2a). In contrast, when the Ag/CNT mixture was heated at a temperature higher than 170 °C, the surface resistance was sufficiently low to illuminate the LED bulbs (Figure 2b, c).

Surface Morphologies of Ag/CNT Films. The changes in the electrical properties of the hybrids can be related to the modifications in their surface shape and structure,[38] which were elucidated using a FE-SEM. The surface morphologies of pristine CNTs and the Ag/CNT hybrid films with different thermal treatments are shown in Figure 3. Pristine CNTs with diameters of 40−60 nm and length of 0.5−10 μm showed entanglements (Figure 3a). When an organic dispersant was used to promote interactions between the CNTs and the AgNPs, the surface morphology was too smooth to obtain a sufficiently high electrical conductivity. A requisite step to increase the surface conductivity was the removal of the insulating POE-imide. Figure 3c−e show the morphologies of the Ag/CNT generated when samples of the POE-imide composite with Ag/CNT were solution-coated on polyimide slides and continuously heated at various temperatures (160, 170, and 350 °C) for 20 min. Results of the control experiment showed that a CNT/POE-imide film exhibited a smooth black surface; the results also showed an unclear image of organic dispersant-wrapped CNTs (Figure 3b). In the presence of AgNPs, when the Ag/CNT in the POE-imide film was heated at 160 °C, the AgNPs migrated and aggregated, resulting in the formation of clusters with a size distribution in the range of 100−150 nm (Figure 3c). When the temperature was increased to 170 °C, the melting of AgNPs into larger lumps was observed, as shown in Figure 3d. When the temperature was further increased to 350 °C, many holes were observed between the melted AgNPs and the CNTs, which indicated that the content of the organic dispersant decreased (Figure 3e). WAXRD analysis (Figure 3f) showed peaks corresponding to four main crystallographic planes, namely, Ag(111), Ag(200), Ag(220), and Ag(311), which indicated that the reduced AgNPs were stable and moved to the film surface. These films containing AgNPs were also examined by TM-AFM. As observed topographically in Figure 4a and d, melted lumps of AgNPs were present on the surface of the films; these lumps had diameters of about 300−500 and 350−800 nm after the films were heated at 170 and 350 °C, respectively, in contrast to the smaller lumps measured by TEM (8−30 nm) (see Figure S1 in the Supporting Information). The phenomenon of particles melting into large lumps is vividly represented in the TM-AFM 3D micrographs shown in Figure 4c, f. These observations are consistent with the FE-SEM observations. Furthermore, in the TM-AFM phase images (Figure 4b, e), a layered structure for the Ag/CNT in the polymer film was observed after the film was heated at both temperatures, perhaps because of the melting of AgNPs on the CNT surfaces at the bottom of the nanohybrid film. The continuous network illustrated the advantage of using melted AgNPs as effective conducting fillers to enhance the conductivity of hybrid materials.

Thermal Degradation of Organic Dispersant during the Annealing of Nanohybrids. The thermal degradation of

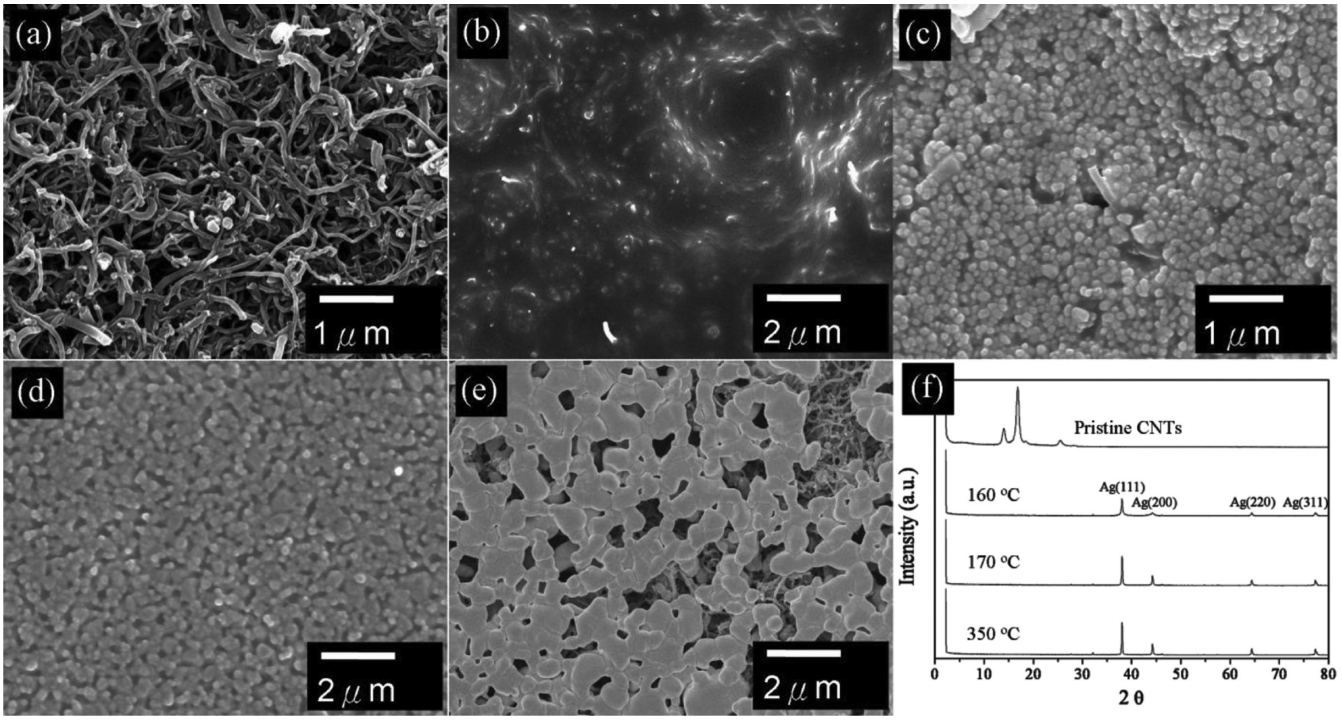

Figure 3. FE-SEM micrographs of (a) pristine CNT; (b) CNT:POE-imide hybrids with a weight ratio of 1:20, dried at 170 °C; (c) CNT:$AgNO_3$:POE-imide hybrids with a weight ratio of 1:20:20, dried at 160 °C; (d) 170 °C; and (e) 350 °C on polyimide substrate. (f) Composition of these samples was examined by WAXRD.

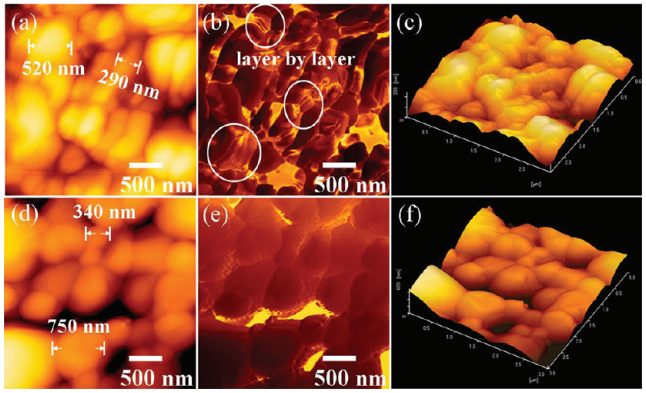

Figure 4. TM-AFM micrographs of the Ag/CNT granules on film surface of (a) topographical, (b) phase micrographs, and (c) 3D micrographs, dried at 170 °C, and (d) topographical, (e) phase micrographs, and (f) 3D micrographs, dried at 350 °C on polyimide substrate.

the organic POE-imide dispersed Ag/CNT nanohybrids was characterized by TGA, as shown in Figure 5. The pristine CNT

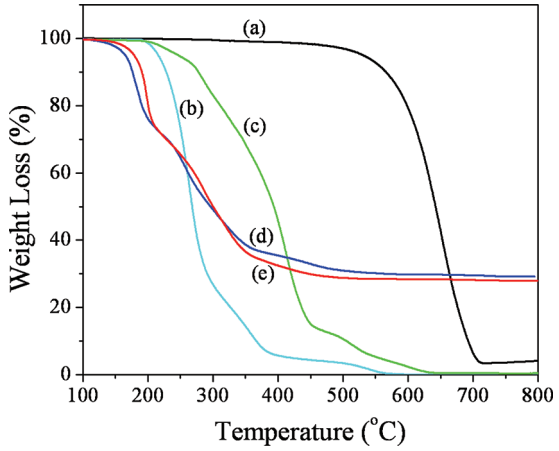

Figure 5. Relative thermo-oxidative stability by TGA in air: (a) pristine CNT, (b) POE-imide (organic dispersant), (c) 5 wt % CNT in POE-imide matrix, (d) POE-imide nanocomposite with AgNP/CNT (CNT:$AgNO_3$:POE-imide weight fraction of 1:20:20), and (e) AgNP/POE-imide ($AgNO_3$:POE-imide weight fraction of 1:1).

exhibited high thermal stability up to 550 °C and degradation over 730 °C. The POE-imide/CNT dispersion had a 10 wt % loss temperature at 280 °C, which was at least 50 °C higher than that of the pure POE-imide in an atmosphere of air. This difference resulted from the fact that the CNTs were dispersed by POE-imide to possess a greater surface area, which led to a considerable increase in the thermal decomposition temperature. In addition, AgNPs had a significant catalytic and oxidative decomposition effects on the organic dispersant matrix at a high temperature.[37] The incorporation of AgNPs into the POE-imide reduced its decomposition temperature, irrespective of the CNTs. Apparently, the POE-imide dispersant had lowered the thermal stability when interacting with AgNP/CNT and AgNPs. The stability temperature at 10 wt % organic weight loss by the standard thermal degradation pattern advanced 60 and 40 °C for the samples with and without CNT, respectively (Figure 5c–e).

Mechanism of Forming Nanohybrid Film with High Conductivity. The formation of a continuous Ag/CNT network on the PI film surface was attributed to high electrical conductivity (Table 1). CNT and AgNP dispersion was contributed to the network formation. The organic dispersant, i.e., POE-imide, possessing the PEO backbone can serve as a reducing agent for converting Ag^+ to Ag^0 and help in the in situ agglomeration into AgNPs, as well as act as a dispersant for CNTs in DMF/water mixtures. The overall fabrication process by solution casting, stepwise heating and Ag migration onto the film surface is conceptually illustrated in Scheme 1.

Scheme 1. Conceptual Illustration of the Overall Process Making Polymer-Dispersed CNT-AgNPs Nanohybrids, Casing, Stepwise Heating, and Ag Migration to Film Surface

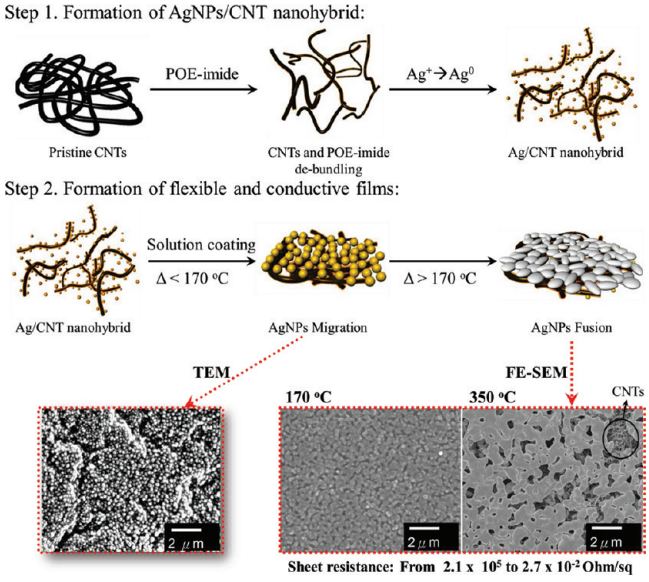

A homogeneous organic solution with Ag/CNT was cast on the PI matrix and then subjected to a series of thermal treatments. The average size of the silver crystals estimated by TEM was no more than 30 nm at ambient temperature (see Figure S1 in the Supporting Information). After annealing 160 °C for 20 min, the TEM micrographs showed particle movement on the CNT surface and a distribution of larger silver particles ranging between 100 and 150 nm in diameter, which resulted from solvent evaporation and POE-imide stretching at high temperature. After increasing the temperature to 170 °C and held there for 20 min, the surface of the finally cured film showed a clear golden color and the sheet resistance showed a critical reduction. It was speculated that this result could be attributed to the catalytic decomposition effect of silver particles, as observed by TGA (Figure 5), as well as to the aggregation of silver particles into larger lumps, as revealed by FE-SEM (Figure 3d). After heating to 350 °C and held there for 20 min, a whitish film was formed and analyzed to be a thin layer (ca. 0.5 μm) of a dense silver network on the film surface due to complete degradation of the organic dispersant. Figure 6a shows the surface of the Ag/CNT film after annealing at 350 °C, exhibiting the Ag melted into an interconnected network. As shown in Figure 6b–d, the film surface was analyzed for the Ag/C, Ag, and C composition by EDX mapping, respectively. The appearance of the interconnected Ag network on the film surface can be correlated the high electric surface conductivity of the film. Besides the surface analyses, the film cross-section was directly identified for the carbon and silver elemental distribution by EDX spectrometry, as shown in Figure 7.

dx.doi.org/10.1021/am2016969 | ACS Appl. Mater. Interfaces 2012, 4, 1449–1455

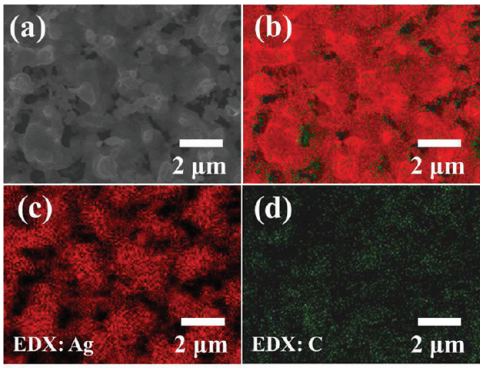

Figure 6. Film surface of CNT:$AgNO_3$:POE-imide (1:20:20 by weight), annealed at 350 °C; (a) FE-SEM, (b) EDX mapping (carbon in green and silver in red), (c) EDX of silver (red), and (d) EDX of carbon (green).

When heating higher than 350 °C, the cross-sectional Ag/CNT film showed the inhomogeneity and generation of porosity on the separated bottom layers, perhaps generated by the POE-imide decomposition. Furthermore, EDX spectrometry showed a very low silver concentration on the bottom layer and a high silver concentration on the top surface (Figure 7d). This is consistent with the observations by FE-SEM and TM-AFM showing that the grain size of the grown silver melt was 350−800 nm. The heating accelerated the melting of the silver, and more importantly, in the presence of oxygen, induced silver-catalyzed polymer degradation to yield a conductive surface. We also assume that the role of CNT is to generate paths for directing the AgNP migration onto the surface. During the heating at 170 °C, there were still some AgNPs attached on the CNT surface, judged by the high conductivity and the presence of Ag and carbon traces by FE-SEM analyses. These above-mentioned proofs should be enough to support our mechanism of silver migration and melt at high temperature. By controlling the stages of thermal treatment, we obtained conductive films with different sheet resistances. Thus, excellent conductivity was achieved as a result of the positive effect of the silver melt.

CONCLUSIONS

The POE-imide dispersant was essential for debundling CNTs and homogeneously dispersing AgNPs in a DMF/water medium. The in situ formation of AgNPs in association with the surfaces of the CNTs became the networks after a simple coating onto a PI substrate and heating. A flexible and conductive Ag/CNT layer on PI films was prepared and showed high surface conductivity of up to 1×10^{-1} Ω/sq and 1×10^{-2} Ω/sq under continuous annealing. In the presence of CNT networks, fine silver particles migrated and aggregated to generate a highly conductive surface. When the Ag/CNT film was heated at 170 °C, the POE-imide decomposed rapidly to allow the silver aggregation into the interconnected network on the surface of the polymer films, which resulted in a surface

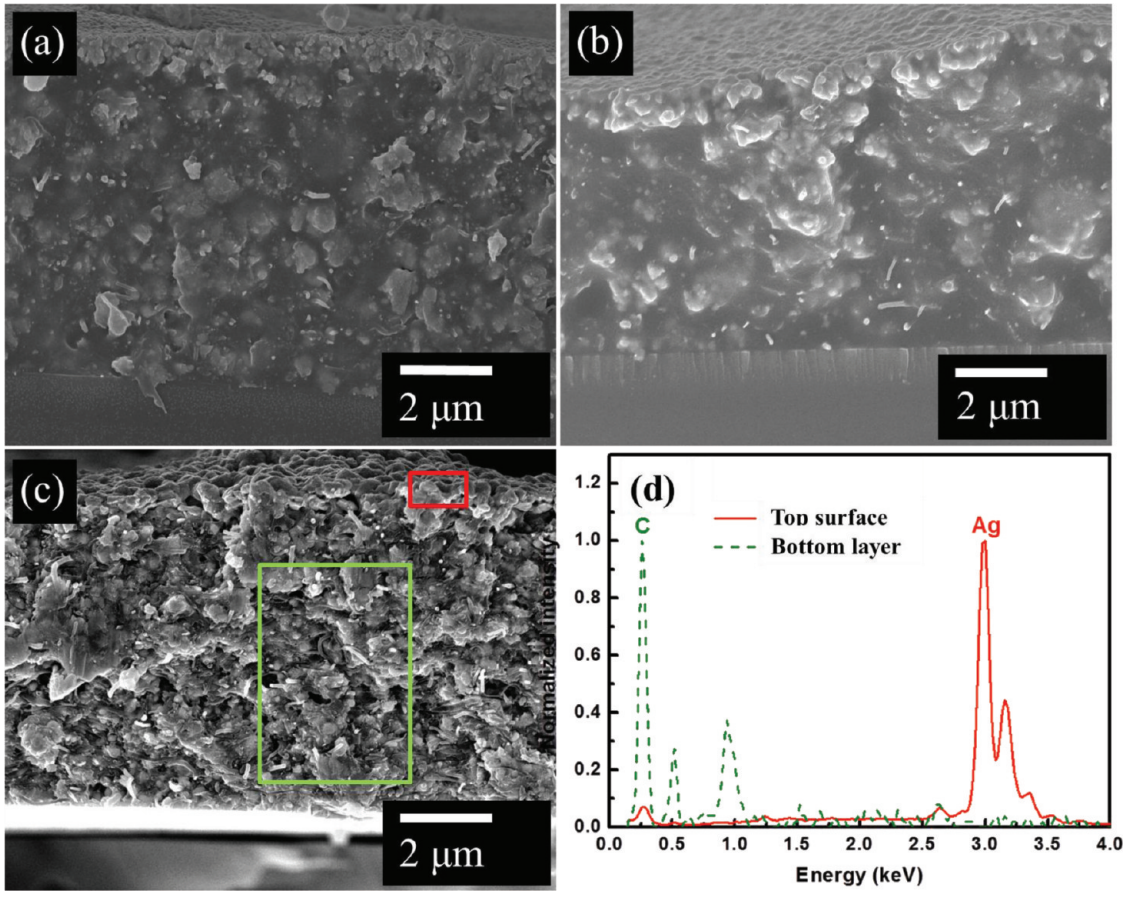

Figure 7. FE-SEM of the cross-sectional view of CNT:$AgNO_3$:POE-imide composite film (1:20:20 by weight; 10 μm), annealed at (a) 160, (b) 170, and (c) 350 °C; (d) energy-dispersive X-ray spectrometry (EDX) analysis, composition of silver and carbon distribution on top surface and bottom layer of film cross-section.

dx.doi.org/10.1021/am2016969 | ACS Appl. Mater. Interfaces 2012, 4, 1449−1455

resistance of 2.0 × 10^{-1} Ω/sq. With a further increase in temperature to 350 °C, the conductivity increased by another order of magnitude. The range of sheet resistance could be controlled by using POE-imide as dispersant for CNTs (1 × 10^{2} Ω/sq) and Ag/CNT (1 × 10^{-1} and 1 × 10^{-2} Ω/sq), thus showing their potential use as nanoconductors for electronic devices.

■ ASSOCIATED CONTENT

Supporting Information

TEM of the Ag/CNT/POE-imide hybrid dispersion. This material is available free of charge via the Internet at http://pubs.acs.org.

■ AUTHOR INFORMATION

Corresponding Author

*Tel: +886-2-3366-5312. Fax: +886-2-2363-8076;. E-mail: jianglin@ntu.edu.tw.

Notes

The authors declare no competing financial interest.

■ ACKNOWLEDGMENTS

We acknowledge financial supports from the National Taiwan University, the Ministry of Economic Affairs and the National Science Council (NSC) of Taiwan under Contract.

■ REFERENCES

(1) Wang, Y.; Tran, H. D.; Liao, L.; Duan, X.; Kaner, R. B. *J. Am. Chem. Soc.* **2010**, *132*, 10365−10373.
(2) Al-Saleh, M. H.; Sundararaj, U. *Carbon* **2009**, *47*, 2−22.
(3) Mendez, J. D.; Weder, C. *Polym. Chem.* **2010**, *1*, 1237−1244.
(4) McEuen, P. L.; Fuhrer, M. S.; Park, H. *IEEE Trans. Nanotechnol.* **2002**, *1*, 78−85.
(5) Badaire, S.; Poulin, P.; Maugey, M.; Zakri, C. *Langmuir* **2004**, *20*, 10367−10370.
(6) Hennrich, F.; Krupke, R.; Arnold, K.; Rojas Stütz, J. A.; Lebedkin, S.; Koch, T.; Schimmel, T.; Kappes, M. M. *J. Phys. Chem. B* **2007**, *111*, 1932−1937.
(7) Dresselhaus, M. S.; Dresselhaus, G.; Eklund, P. C. *Science of Fullerenes and Carbon Nanotubes*; Academic: London, 1996.
(8) Blanch, A. J.; Lenehan, C. E.; Quinton, J. S. *J. Phys. Chem. B* **2010**, *114*, 9805−9811.
(9) Datsyuk, V.; Landois, P.; Fitremann, J.; Peigney, A.; Galibert, A. M.; Soula, B.; Flahaut, E. *J. Mater. Chem.* **2009**, *19*, 2729−2736.
(10) Campbell, J. F.; Tessmer, I.; Thorp, H. H.; Erie, D. A. *J. Am. Chem. Soc.* **2008**, *130*, 10648−10655.
(11) Wu, Z.; Zhen, Z.; Jiang, J. H.; Shen, G. L.; Yu, R. Q. *J. Am. Chem. Soc.* **2009**, *131*, 12325−12332.
(12) Simmons, T. J.; Bult, J.; Hashim, D. P.; Linhardt, R. J.; Ajayan, P. M. *ACS Nano* **2009**, *3*, 865−870.
(13) Yao, Q.; Chen, L.; Zhang, W.; Liufu, S.; Chen, X. *ACS Nano* **2010**, *4*, 2445−2451.
(14) Blake, R.; Coleman, J. N.; Byrne, M. T.; McCarthy, J. E.; Perova, T. S.; Blau, W. J.; Fonseca, A.; Nagy, J. B.; Gun'ko, Y. K. *J. Mater. Chem.* **2006**, *16*, 4206−4213.
(15) Baykal, B.; Ibrahimova, V.; Er, G.; Bengü, E.; Tuncel, D. *Chem. Commun.* **2010**, *46*, 6762−6764.
(16) Tang, B. Z.; Xu, H. Y. *Macromolecules* **1999**, *32*, 2569−2576.
(17) Star, A.; Gabriel, J. C. P.; Bradley, K.; Gruner, G. *Nano Lett.* **2003**, *3*, 459−463.
(18) Freitag, M.; Martin, Y.; Misewich, J. A.; Martel, R.; Avouris, P. H. *Nano Lett.* **2003**, *3*, 1067−1071.
(19) Stauffer, D.; Aharony, A. *Introduction to Percolation Theory*; Taylor and Francis: London, 1992.
(20) Sandler, J. K. W.; Kirk, J. E.; Shaffer, M. S. P.; Windle, A. H. *Polymer* **2003**, *44*, 5893−5899.
(21) Bryning, M. B.; Islam, M. F.; Kikkawa, J. M.; Yodth, A. C. *Adv. Mater.* **2005**, *17*, 1186−1191.
(22) Grossiord, N.; Loos, J.; Regev, O.; Koning, C. E. *Chem. Mater.* **2006**, *18*, 1089−1099.
(23) Winey, K. I.; Kashiwagi, T.; Mu, M. *MRS Bull.* **2007**, *32*, 348−353.
(24) Arnold, A.; Hennrich, F.; Krupke, R.; Lebedkin, S.; Kappes, M. M. *Phys. Status Solidi B* **2006**, *243*, 3073−3076.
(25) Wang, Z.; Liu, Q.; Liu, H.; Chen, Y.; Yang, M. *Carbon* **2007**, *45*, 285−292.
(26) Benoit, J. −M.; Corraze, B.; Lefrant, S.; Blau, W. J.; Bernier, P.; Chauvet, O. *Synth. Met.* **2001**, *121*, 1215−1216.
(27) Kymakis, E.; Amaratunga, G. A. J. *J. Appl. Phys.* **2006**, *99*, 084302.
(28) Marsh, D. H.; Rance, G. A.; Whitby, R. J.; Giustiniano, F.; Khlobystov, A. N. *J. Mater. Chem.* **2008**, *18*, 2249−2256.
(29) Ma, P. C.; Tang, B. Z.; Kim, J. K. *Carbon* **2008**, *46*, 1497−1505.
(30) Ren, G.; Xing, Y. *Nanotechnology* **2006**, *17*, 5596−5601.
(31) Oh, Y.; Chun, K. Y.; Lee, E.; Kim, Y. J.; Baik, S. *J. Mater. Chem.* **2010**, *20*, 3579−3582.
(32) Chun, K. Y.; Oh, Y.; Rho, J.; Ahn, J. H.; Kim, Y. J.; Choi, H. R.; Baik, S. *Nat. Nanotechnol.* **2010**, *5*, 853−857.
(33) Guo, D. J.; Li, H. L. *Carbon* **2005**, *43*, 1259−1264.
(34) Su, H. L.; Chou, C. C.; Hung, D. J.; Lin, S. H.; Pao, I. C.; Lin, J. H.; Huang, F. L.; Dong, R. X.; Lin, J. J. *Biomaterials* **2009**, *30*, 5979−5987.
(35) Untereker, D.; Lyu, S.; Schley, J.; Martinez, G.; Lohstreter, L. *ACS Appl. Mater. Interfaces* **2009**, *1*, 97−101.
(36) Southward, R. E.; Thompson, D. W. *Chem. Mater.* **2004**, *16*, 1277−1284.
(37) Qi, S.; Wu, Z.; Wu, D.; Wang, W.; Jin, R. *Chem. Mater.* **2007**, *19*, 393−401.
(38) Qi, S.; Wu, Z.; Wu, D.; Wang, W.; Jin, R. *Langmuir* **2007**, *23*, 4878−4885.
(39) Yang, N.; Aoki, K.; Nagasawa, H. *J. Phys. Chem. B* **2004**, *108*, 15027−15032.
(40) Ding, X.; Xu, R.; Liu, H.; Shi, W.; Liu, S.; Li, Y. *Cryst. Growth Des.* **2008**, *8*, 2982−2985.
(41) Yao, H. B.; Huang, G.; Cui, C. H.; Wang, X. H.; Yu, S. H. *Adv. Mater.* **2011**, *23*, 3643−3647.
(42) Dong, R. X.; Chou, C. C.; Lin, J. J. *J. Mater. Chem.* **2009**, *19*, 2184−2188.
(43) Huang, K. C.; Wang, Y. C.; Dong, R. X.; Tsai, W. C.; Tsai, K. W.; Wang, C. C.; Chen, Y. H.; Vittal, R.; Lin, J. J.; Ho, K. C. *J. Mater. Chem.* **2010**, *20*, 4067−4073.